A&A 415, 521–529 (2004)
DOI: 10.1051/0004-6361:20034633

Astronomy & Astrophysics

BVRIJK light curves and radial velocity curves for selected Magellanic Cloud Cepheids⋆,⋆⋆

J. Storm[1], B. W. Carney[2], W. P. Gieren[3], P. Fouqué[4,5], W. L. Freedman[6], B. F. Madore[7], and M. J. Habgood[2]

[1] Astrophysikalisches Institut Potsdam, An der Sternwarte 16, 14482 Potsdam, Germany
[2] Univ. of North Carolina at Chapel Hill, Dept. of Physics and Astronomy, Phillips Hall, Chapel Hill, NC-27599-3255, USA
e-mail: bruce@physics.unc.edu
[3] Universidad de Concepción, Departamento de Física, Casilla 160-C, Concepción, Chile
e-mail: wgieren@coma.cfm.udec.cl
[4] Observatoire de Paris, Section de Meudon DESPA, 92195 Meudon Cedex, France
[5] European Southern Observatory, Casilla 19001, Santiago 19, Chile
e-mail: pfouque@eso.org
[6] The Observatories, Carnegie Institution of Washington, 813 Santa Barbara Street, Pasadena, Ca 91101, USA
e-mail: wendy@ociw.edu
[7] California Institute of Technology, IPAC, MC 100-22, Pasadena, Ca 91125, USA
e-mail: barry@ipac.caltech.edu

Received 5 August 2003 / Accepted 14 November 2003

Abstract. We present high-precision and well sampled *BVRIJK* light curves and radial velocity curves for a sample of five Cepheids in the SMC. In addition we present radial velocity curves for three Cepheids in the LMC. The low-metallicity ([Fe/H] ≈ -0.7) SMC stars have been selected for use in a Baade-Wesselink type analysis to constrain the metallicity effect on the Cepheid Period-Luminosity relation. The stars have periods of around 15 days so they are similar to the Cepheids observed by the Extragalactic Distance Scale Key Project on the Hubble Space Telescope. We show that the stars are representative of the SMC Cepheid population at that period and thus will provide a good sample for the proposed analysis. The actual Baade-Wesselink analysis is presented in a companion paper.

Key words. Cepheids – Magellanic Clouds

1. Introduction

Recently Freedman et al. (2001) have concluded the Hubble Space Telescope key project on the Extragalactic Distance Scale. They applied the Cepheid Period-Luminosity relation to Cepheids in distant galaxies to calibrate secondary standard candles which in turn can be used to measure the free Hubble flow in the Universe to an accuracy of better than 10%. This result depends on the distance to the Large Magellanic Cloud, which has been assumed to be $(m - M)_0 = 18.5 \pm 0.1$, and on the assumption that the PL relation is only weakly dependent on metallicity. Many studies in the last decade have tried to resolve both of these issues, but widely differing results keep turning up.

In this paper we present data which will be used for a study of the metallicity effect on the PL relation. The idea is to determine the luminosities of individual, low metallicity ([Fe/H] ≈ -0.7), SMC Cepheids and compare these luminosities to those of solar metallicity Galactic Cepheids of similar period. The low metallicity of the SMC Cepheids combined with the solar metallicity Galactic stars provide a reasonably large range in metallicity to place significant constraints on the effect metallicity has on the PL relation.

The recent calibration of the infrared surface brightness method (Fouqué & Gieren 1997) provides a powerful tool for determining luminosities for individual Cepheids. However, to exploit the full potential of the method accurate optical (V-band) and near-IR (K-band) light curves, as well as well-sampled and accurate radial velocity curves are needed. In the present paper we present all the observational data which is needed for the analysis. Preliminary analyses and discussions have already been presented in Storm et al. (1998, 1999 and 2000), and in a companion paper (Storm et al. 2004) we present

Send offprint requests to: J. Storm (AIP), e-mail: jstorm@aip.de

⋆ Based on data acquired at the Las Campanas Observatory, Chile, the Cerro Tololo Inter American Observatory, Chile, and the European Southern Observatory, Chile.

⋆⋆ Tables 10–27 are only available in electronic form at the CDS via anonymous ftp to cdsarc.u-strasbg.fr (130.79.128.5) or via http://cdsweb.u-strasbg.fr/cgi.bin/qcat?J/A+A/415/521

Table 1. The coordinates of the Cepheids as returned by skycat from the Digital Sky Survey (J2000.0).

Identifier	OGLE ID	RA hh:mm:ss	Dec dd:mm:ss
	SMC		
HV 822	SC2-84516	00:41:55.6	−73:32:25
HV 1328		00:32:54.7	−73:49:20
HV 1333		00:36:03.5	−73:55:58
HV 1335	SC1-00001	00:36:55.4	−73:56:30
HV 1345	SC2-41552	00:40:38.5	−73:13:14
	LMC		
HV 2694	SC16-70661	05:35:32.0	−69:43:22
HV 12797		05:22:24.0	−71:59:19
HV 12198		05:13:26.7	−65:27:05

our final surface brightness analysis of the stars and determine the constraints on the metallicity effect on the Cepheid PL relation, and the consequences for the value of the Hubble constant.

Five Cepheids in the south-western part of the SMC about 1 degree from the main body of the galaxy were selected for further study. With this location the stars are representative of the SMC population but not affected by the variable extinction and severe crowding which is found closer to the main body of the SMC. The coordinates for the stars are listed in Table 1. Finding charts can be found in Hodge & Wright (1977). The stars were selected to have periods around 15 days, long enough to avoid overtone pulsators, and to guarantee similarity to Cepheids used for extragalactic distance determination, but still short enough to allow a complete phase coverage with a reasonable number of nights at the telescope. Using a sample of almost equal period stars also allows us to probe the intrinsic width of the instability strip at this period.

In addition to the SMC sample we also observed a few LMC Cepheids of different periods, and for completeness we present the data acquired for these stars here as well.

2. The optical photometric data

2.1. The observations

The Cepheids were observed with a number of CCD cameras at the Las Campanas, Cerro Tololo and La Silla observatories in Chile as summarized in Table 2. The stars were observed in the *BVR* and *I* bands and the exposure times ranged from 30 s to a few minutes depending on the instrument sensitivity, the seeing and the transparency of the sky. The seeing was typically in the range 0.9 to 1.4 arcsec and all frames with seeing worse than about 2 arcsec were discarded as crowding effects started to become significant. In all cases the point spread function (PSF) was well sampled by the detector.

2.2. Data reduction

2.2.1. Pre-processing

The CCD frames were bias-subtracted using a constant value for the bias level determined from bias exposures. The flat fielding was done using sky flatfields for the large-scale structure and dome flatfields for the pixel-to-pixel variations in case of the Las Campanas data. For the CTIO data, the high read-out speed of the detector (about 15 s for a full frame) allowed the exclusive use of sky flatfields for the gain calibration.

The 1989 observing run at Las Campanas was somewhat compromised by significant gain variations of the UV-flooded Texas Instrument CCD during the individual nights. After various experiments we have been reasonably successful in scaling and interpolating the flatfields for each science frame to compensate the effect, but these data are of lower quality than those obtained with the other instruments.

2.2.2. Relative photometry

The relative photometry was determined using the DoPHOT_2.0 package (Schecter et al. 1993). The intermediate photometric system was defined by the CTIO observations from the night of Jan. 2, 1994 as the CTIO system is close to the standard Landolt (1992) system. Furthermore the seeing and photometric quality was good on this night and seven standard field observations were performed (see below).

For each of the other observing runs transformation to the CTIO system of the form

$$v_{\rm ctio} = v_{\rm inst} + \alpha_{vbv} \times (b - v)_{\rm inst} + \text{const.}\,, \quad (1)$$

$$(b - v)_{\rm ctio} = \alpha_{bv} \times (b - v)_{\rm inst} + \text{const.}\,, \quad (2)$$

$$(v - r)_{\rm ctio} = \alpha_{vr} \times (v - r)_{\rm inst} + \text{const.}\,, \quad (3)$$

$$(v - i)_{\rm ctio} = \alpha_{vi} \times (v - i)_{\rm inst} + \text{const.}\,, \quad (4)$$

were determined. The transformations were first determined for each set of instrument magnitudes *bvri* based on the brightest (lowest estimated error) stars in common with the CTIO data. Typically more than 100 stars in each field were used. The coefficients were then averaged over each observing run giving the values listed in Table 2. The typical rms for the color terms is of the order 0.02 mag. These averaged coefficients were then used for the next iteration where only the zero points for the individual frames were fitted. The final transformation of the *bvri* sets to the CTIO system was then performed using these zero points and the average transformation coefficients.

2.2.3. Transformation to the standard system

On the night of Jan. 2, 1994 we observed three Landolt (1992) fields. Each field was observed two or three times at different airmass giving a total of 31 *BVRI* measurements of standard stars covering a wide range in color ($-0.3 < (B-V) < 1.9$) and airmass ($1.1 < X < 1.8$). Synthetic aperture photometry was performed using the IRAF[1] `noao.digiphot.apphot` package and employing an aperture radius of 18 pixels corresponding to a diaphragm diameter of 14 arcsec, which also happens to be very similar to the one employed by Landolt (1992).

[1] IRAF is the Image Reduction and Analysis Facility, made available to the astronomical community by the National Optical Astronomy Observatories, which are operated by AURA, Inc., under cooperative agreement with the National Science Foundation.

Table 2. Coefficients for the transformation of the various instrument systems to the CTIO instrument system.

Observing period	Observatory	Instrument (Detector)	α_{vbv}	α_{bv}	α_{vr}	α_{vi}
Nov. 1988	LCO	1 m (TI#1)	−0.089	1.168	0.890	0.898
Jul. 1989	CTIO	0.9 m (RCA#5)	−0.077	1.177	0.963	0.963
Jul. 1989	CTIO	0.9 m (TI#3)	−0.078	1.112	0.933	0.945
Aug. 1989	CTIO	4 m (TI#1)	−0.071	1.268	0.943	0.937
Nov. 1989	LCO	1 m (TI#2)	−0.089	1.168	0.890	0.898
Dec. 1993	CTIO	0.9 m (Tek#2)	0.000	1.000	1.000	1.000
Jan. 1996	ESO	DFOSC (C1W11/4)	0.032	1.227	0.928	1.022
Jul. 1996	ESO	DFOSC (C1W11/4)	0.032	1.227	0.928	1.022
Jul. 1996	ESO	EFOSC-2 (CCD#40)	0.066	1.076	1.023	1.025
Sep. 1996	ESO	DFOSC (C1W11/4)	0.017	1.097	0.939	1.021
Oct. 1996	CTIO	0.9 m (Tek#3)	−0.009	0.932	0.989	0.982

Table 3. Coefficients for the transformation of the CTIO instrument system to the Landolt (1992) system.

	B	*V*	*R*	*I*
color	$(b-v)$	$(b-v)$	$(v-r)$	$(v-i)$
α_m	0.007	0.019	0.008	0.006
σ_α	0.006	0.003	0.005	0.003
k_m	−0.249	−0.147	−0.118	−0.059
σ_k	0.013	0.007	0.007	0.009
c_m	−4.913	−4.204	−4.183	−5.013
σ_c	0.018	0.010	0.010	0.012
rms	0.018	0.012	0.010	0.012

Table 4. Ephemerides adopted for the stars.

Identifier	Period days	$\log_{10}(P)$	Epoch HJD
HV 822	16.7421	1.223810	2 447 485.9
HV 1328	15.8360	1.199645	2 447 486.7
HV 1333	16.2935	1.212014	2 447 491.3
HV 1335	14.3816	1.157807	2 450 610.6
HV 1345	13.4784	1.129638	2 447 496.0
HV 2694	6.9363	0.841128	2 449 349.4
HV 12797	6.82	0.8338	2 432 000.0
HV 12198	3.5228	0.550573	2 432 011.6

The IRAF `photcal` package was used to derive the transformations in the form

$$M = m + \alpha_m \times \text{color} + k_m \times X + c_m \quad (5)$$

where M refers to standard magnitudes and m to the CTIO instrumental magnitudes, color refers to the instrumental color term ($(b-v)$ or $(v-r)$ or $(v-i)$) as listed in Table 3, k_m is the extinction coefficient for passband m, X is the airmass and c_m is the zero point for passband m.

The values of the coefficients with the estimated errors are listed in Table 3. Note that the CTIO instrument system closely resembles the standard system.

To tie in the instrumental magnitudes from the DoPHOT PSF fitting photometry, $m_{\rm PSF}$, with the aperture photometry of the standard star observations we determined the aperture corrections for the PSF photometry for each individual field. HV 822 was the only field which was not observed during this night, and it was tied in with the HV 1345 field on the following night using a similar procedure.

In the case of HV 1335 it was necessary to add an offset of $\Delta V = -0.1$ mag to the magnitudes from the Nov. 1989 run to bring the V light curve into agreement with that obtained from the other instruments. This is the only deviation from the transformations given above, and it is justified as some of the frames from this run are likely to suffer from residual systematic errors in the flatfielding. The fact that the other stars agree reasonably well with the measurements from the other runs indicate that the flatfielding for the Nov. 1989 run overall has been quite successful.

2.3. Ephemerides

The periods for the stars were re-derived from the present data by minimizing the dispersion between the points in the V-band light curve. The epoch of maximum V-light was finally determined by shifting the light curve by eye to obtain a good fit. For HV 1335 we have adopted the values found by Udalski et al. (1999). The adopted ephemerides are listed in Table 4.

2.4. The light curves

The photometry for the stars is given in Tables 10–14 together with the photometric errors as returned by DoPHOT. The light curves are plotted in Fig. 1 where the different observing runs are indicated by a different symbol. The phases were determined on the basis of the ephemerides from Table 4.

2.5. Comparison with other sources of photometry

Caldwell & Coulson (1984) presented photoelectric photometry for HV 1335. We find excellent agreement with their light curve when we add an offset of +0.07 mag to their V magnitudes. Such an offset is expected as HV 1335 has two faint ($\Delta V \approx 3.5$) companions within a distance of 5 arcsec which will make the aperture photometry (which includes the two companions) brighter by approximately the observed amount.

Laney & Stobie (1994) quote mean V magnitudes for the two stars HV 1328 and HV 1335 but again based on photoelectric measurements so a precise agreement cannot be expected

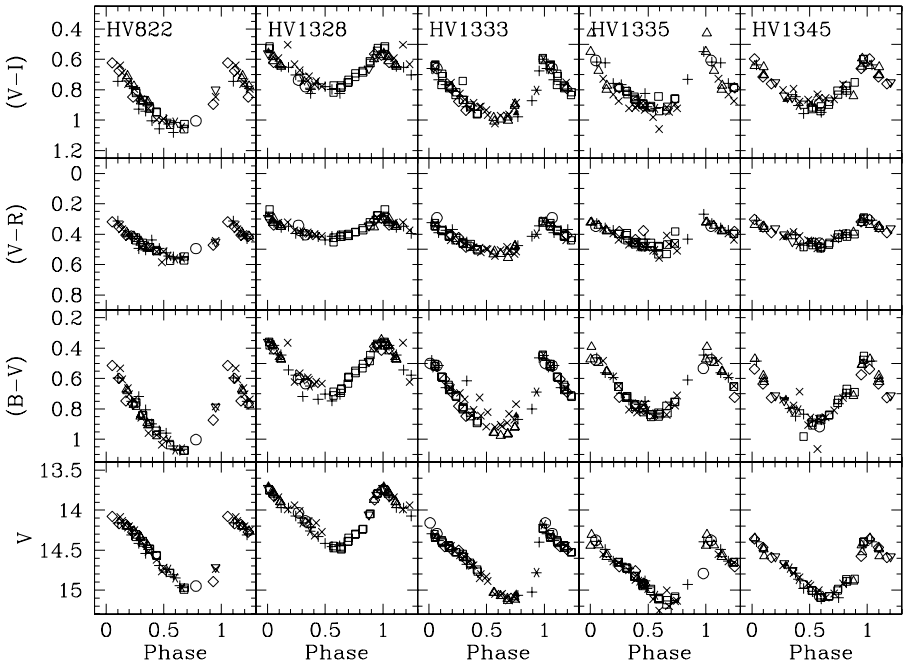

Fig. 1. Light and color curves for the SMC Cepheids. The data are marked in the following way: plusses: LCO 1988, crosses: LCO 1989, open diamonds: CTIO 1989, open squares: CTIO 1993, open inverse triangles: DFOSC Jan. 1996, filled triangles: DFOSC Jul. 1996, open circles: EFOSC-2 Jul. 1996, open triangles: DFOSC Sep. 1996, asterisks: CTIO 1996.

due to contamination within either the object aperture or the sky aperture.

More recently Udalski et al. (1999) (The OGLE SMC Cepheid database) have published CCD-based *BVI* light curves for three of the stars presented here, namely HV 822, HV 1335 and HV 1345. For each of these stars they have about 10 *B*-band, 25 *V*-band, and 150 *I*-band observations with good phase coverage. The agreement with the photometry presented here is good with the zero points agreeing to better than 0.01 mag suggesting that our photometric zero-point is accurate to about 0.01 mag. The only offsets which we have deemed necessary are in the *I*-band where we have offset their photometry for HV 822 by +0.02 mag and for HV 1335 by +0.03 mag before we determined the mean value.

In Fig. 2 the OGLE *V*-band light curve for HV 822 has been overplotted on our measurements. The agreement is excellent even though the intensity means of the two data sets differ by 0.05 mag. This difference is, however, mainly due to a different phase coverage especially in the phase range 0.8 to 1.0 where the magnitudes change rapidly and where the light curve exhibits several inflection points.

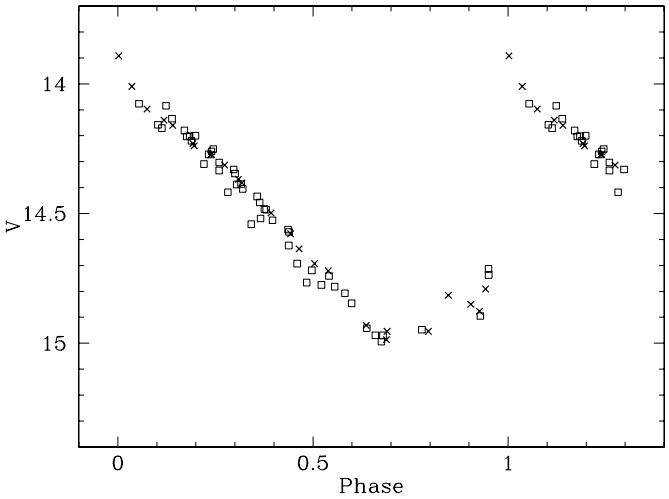

Fig. 2. The *V*-band light curve for HV 822 (open boxes) from our data with the measurements from Udalski et al. (1999) overplotted (crosses).

3. The near-IR data

J and *K*-band data were acquired for the five SMC stars with a variety of instruments as tabulated in Table 5. As the periods of the stars are so long, it only made sense to obtain one or at most two phase points per night. With the limited number of stars in the sample it was possible to obtain these data within a short time in parallel to the main observing program (Cepheids in young LMC clusters).

3.1. Data reduction

The observations were made in a five-position dither mode enabling a sky frame to be constructed by median filtering these dithered frames. This local sky was subtracted from the individual science frames which were then flatfielded by an appropriate flatfield. The flatfield was either made from twilight exposures with an appropriate dark frame subtracted (Las Campanas) or from dome flats where high- and low-light intensity frames with identical exposure time were subtracted from each other (ESO and CTIO).

Table 5. List of observing runs which contributed to the near-IR data set.

Date	Observatory	Instrument
Jan. 1998	ESO, La Silla	2.2 m with IRAC-2
Oct. 1998	Las Campanas	1.0 m with C40IRC
Dec. 1998	Las Campanas	2.5 m with IRCAM
Jan. 1999	Las Campanas	1.0 m with C40IRC
Jan. 1999	Las Campanas	2.5 m with IRCAM
Jan. 2000	CTIO	1.5 m with OSIRIS

A linearity correction was applied to the raw frames where appropriate, but all science and calibration frames were obtained with sufficiently low count levels, so the non-linearity does not affect the data (<1% correction).

3.2. Photometry

The photometry was done using the PSF fitting program DAOPHOT-II (Stetson 1987) within IRAF. An instrumental photometric system was defined for each field by a set of exposures obtained on a night of good photometric quality. All the frames for the field from the other nights and other instruments were transformed to this system in a manner similar to the process described in a previous section for the optical data. Color terms were determined between the instrumental system and the other instruments on the basis of photometry of stars in the young LMC cluster NGC 2136 with a wide range of $(J-K)$ color. In all cases no significant color term between the instrument systems could be established at the 2% level.

3.3. Calibration to the standard system

During the nights Dec. 27 and Dec. 28 1998, we observed eight standard stars several times for a total of 21 standard star observations. The stars were all from the list of Persson et al. (1998) and span the color range from $(J-K) = 0.24$ to 0.95. Each observation consisted of four dithered exposures in each of the J and Ks filters. The airmass terms were determined to be similar to the canonical values ($k_J = 0.10$, $k_K = 0.08$) adopted by Persson et al. (1998) so we adopted these values. We also, as expected, did not detect a color term with respect to the Persson system so we only had to determine the nightly zero points. For the reddest measurements ($(J-K) > 0.45$) we applied the transformation determined by Persson et al. (1998) to transform the data to the CIT system, otherwise the two systems were considered identical.

On the same nights the science fields were also observed, and tertiary reference stars in the fields were tied in with the standard system by applying the offsets determined for the standard stars and correcting for the appropriate airmass term. This was done using the IRAF package `photcal` on synthetic aperture photometry of isolated stars in the fields and using growth curves to take out any variation which might be present due to seeing variations.

The observations from the other nights were offset to the Las Campanas instrument system as described in the previous section and these transformed data were finally transformed to the CIT system using the zero points offsets determined here. The resulting photometry is tabulated in Tables 15–19.

3.4. The K-band light curve and $(J-K)$ and $(V-K)$ color curves

The main purpose of the near-IR observations is to obtain a well defined $(V-K)$ color curve for each Cepheid which is necessary for the application of the near-IR surface brightness relation to these stars. At the same time we can obtain good J and K light curves and thus a good estimate of the mean J- and K-band magnitudes of the stars, for comparison with the corresponding Cepheid PL relations. The $(J-K)$ color curve can potentially also be used for a Baade-Wesselink type analysis, but for these stars it turns out that the amplitude is very small and thus the photometric uncertainties become significant. In short, the $(J-K)$ color is a poor (insensitive) temperature indicator for these stars.

We have compared our K-band photometry with the measurements by Welch et al. (1987) and find excellent agreement. Their (few) points have been overplotted in the K-band light curves and will be used in the determination of the $(V-K)$ color curve.

As the near-IR data were obtained at different times from the V-band observations it is necessary to construct the $(V-K)$ color curve on the basis of the V and K-band light curves, i.e. in phase space. As the observations are not obtained at exactly the same phases, it is necessary to interpolate to obtain the color at a given phase. We decided to do this by fitting a 3rd or 4th order Fourier series to the K-band data and then use this expansion to compute the corresponding K value for each V phase point. The K-band light curve has the lowest amplitude (±0.15 mag) and is significantly more sinusoidal than the V-band light curve, and thus lends itself well to a low-order Fourier fit. The low-order fits follow the general trend of the light curves rather well and the possible errors introduced from the fit are small. Of course there is an enhanced uncertainty where the phase coverage is poor. We have tried to use different (reasonable) orders for the fits but the resulting Baade-Wesselink results were not affected significantly. The Fourier fit to the data points has been overplotted in Figs. 3–7.

To obtain the best possible phase coverage we have combined our V-band data with those of Udalski et al. (1999). No offsets have been applied as we could not determine any offset with a significance of more than 0.01 mag.

The resulting $(V-K)$ color curves are shown in Fig. 8 and the photometric values are tabulated in Table 20–24. We note that one point on the $(V-K)$ curve for HV 1335 at phase 0.979 is significant fainter than the neighbouring points. We assume that this is a deviant point and not an indication of a possible phase mismatch. In the Baade-Wesselink analysis we will anyway disregard the phase region from 0.8 to 1.0 as will be discussed in Storm et al. (2004).

4. The radial velocities

The radial velocity curves were determined from Echelle spectra obtained with the Las Campanas Observatory 2.5 m Du Pont

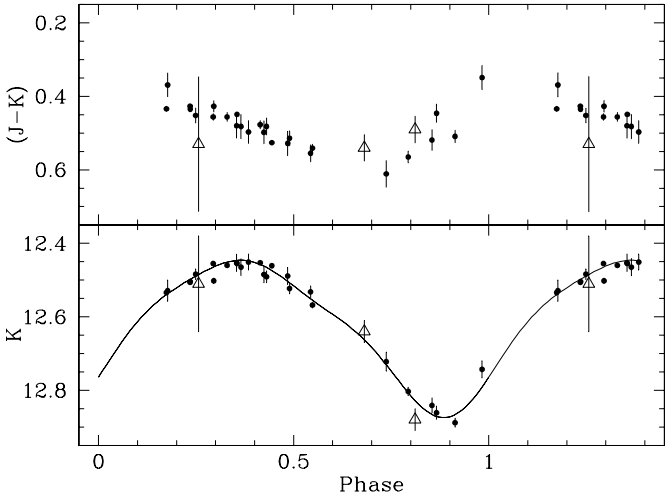

Fig. 3. Near-IR light and color curves for HV 822. Open triangles are from Welch et al. (1987).

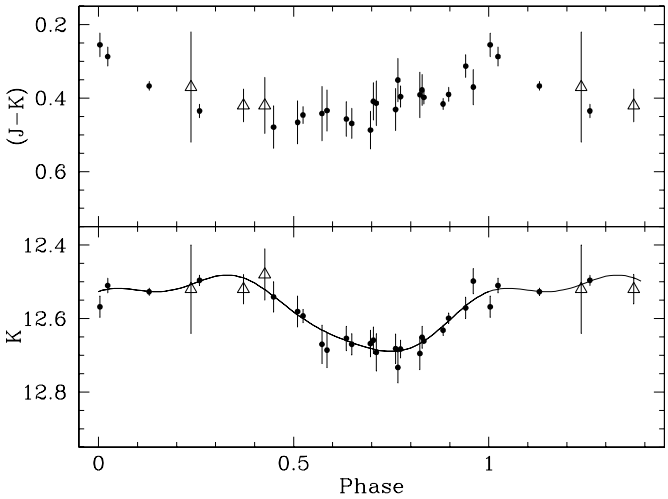

Fig. 4. Near-IR light and color curves for HV 1328. Open triangles are from Welch et al. (1987).

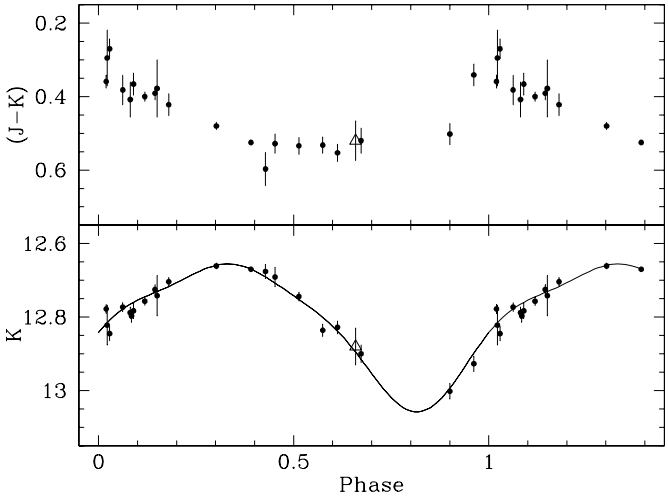

Fig. 5. Near-IR light and color curves for HV 1333. Open triangles are from Welch et al. (1987).

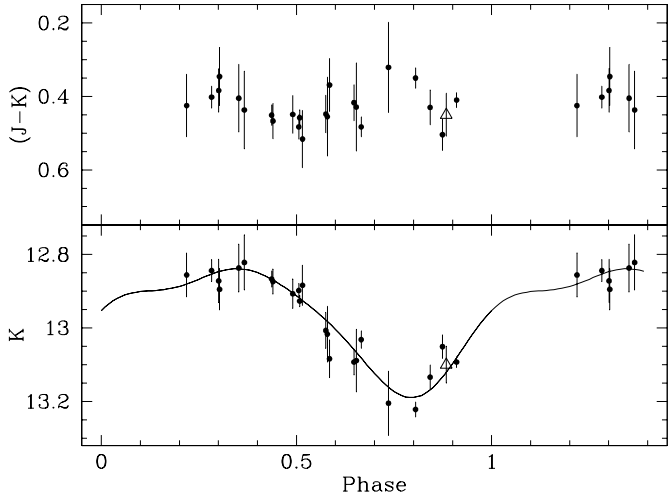

Fig. 6. Near-IR light and color curves for HV 1335. Open triangles are from Welch et al. (1987).

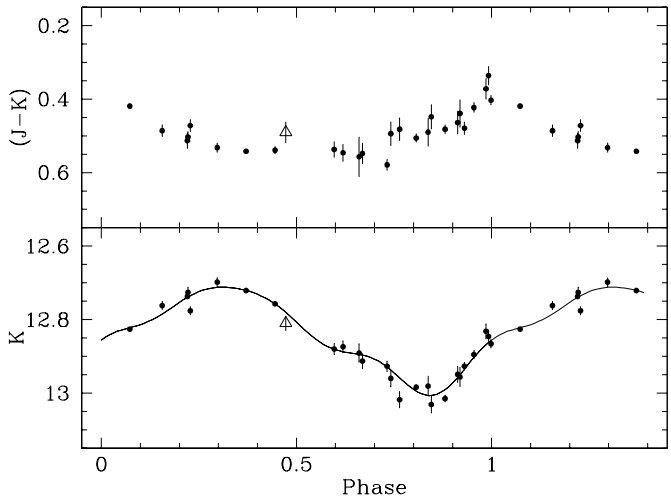

Fig. 7. Near-IR light and color curves for HV 1345. Open triangles are from Welch et al. (1987).

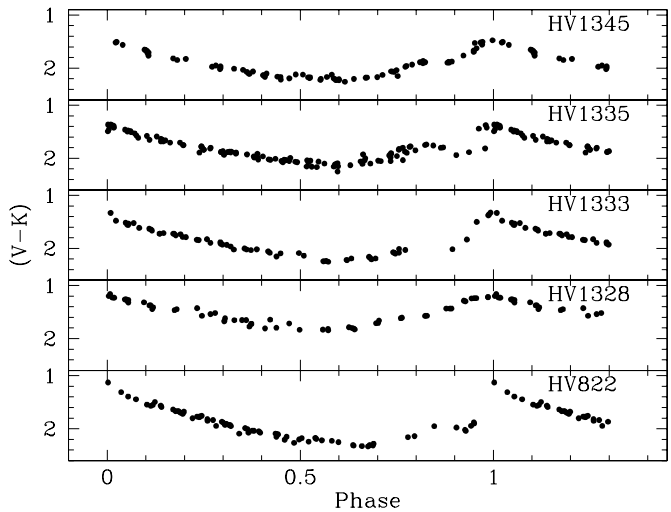

Fig. 8. The $(V - K)$ color curves for the five prime targets.

telescope equipped with the echelle spectrograph and the 2D-Frutti photon counting system.

The spectrograph provides a dispersion of 0.2 nm/mm (≈0.006 nm pix^{-1}) and was used with a slit of 1.5 × 4 arcsec which transforms into an instrumental profile with a *FWHM* of approximately 3.5 pixels or 12 km s^{-1}. The spectrograph is very efficient for our purpose, providing typical signal-to-noise ratios of 10 per resolution element with exposure times ranging from 30 to 60 min depending on the brightness of the object.

Additional measurements were secured with the ESO Multi-Mode Instrument (EMMI) mounted at the ESO New Technology Telescope (NTT) at the La Silla Observatory. The red arm of the instrument with a CCD detector (Loral #34) was used with the echelle grating #10 giving a dispersion of 0.24 nm/mm. The efficiency was not quite as high as for the Las Campanas instrument, but similar S/N ratios could be obtained with similar exposure times.

4.1. Observations

The Las Campanas data were obtained during four observing runs in the seasons 1987, 1988, 1989 and 1994 and comprise 171 science spectra for the objects described here. The La Silla data were obtained during technical time on one night in October 1992 and a few nights in September 1993 and add an additional 8 velocity measurements. The exact timing of the exposures is listed together with the resulting radial velocities in Table 25 and 26.

Reference Th-Ar exposures of 600 s were obtained just before or after each of the scientific exposures. As radial velocity reference we observed the twilight sky as well as the star C349 in 47 Tuc (chart in Chun & Freeman 1978). 47 Tuc is conveniently located near the SMC so the instrument is pointing in almost the same direction as during the science exposures, thus minimizing any differential flexure and ensuring a minimum overhead of observing time.

4.2. Data reduction

The echelle spectra were reduced and analysed using IRAF.

The raw data frames were flat-fielded using an average flat-field for each observing run which had the large-scale structure removed and which was normalized. In this way the statistical properties of the data were largely maintained.

The IRAF package `noao.imred.echelle` was used for extracting the orders and for performing the wavelength calibration. Due to limited computing power at the beginning of the project, 10 orders covering the range $\lambda\lambda$ 475–555 nm were used for the first three runs and for the Nov. 1994 run 20 orders covering the range $\lambda\lambda$ 417–555 nm were used. For the NTT data the range $\lambda\lambda$ 490–640 nm was used.

Th-Ar exposures obtained immediately before or immediately after the science exposure with the telescope in the same position were employed for defining the wavelength solution.

The resulting one-dimensional spectra were then fed into the cross-correlation program `XCOR` (for a description see Morse et al. 1991) and for the later runs the related program `XCSAO` (Kurtz et al. 1992) which is part of the `RVSAO` package for IRAF. The algorithms are based on the technique described by Tonry & Davis (1979).

Table 6. Radial velocities for the reference star 47 Tuc-C349 measured with respect to the twilight sky.

HJD	Rad. vel. km s^{-1}
2 449 234.7919	−20.6
2 449 237.7682	−20.3
2 449 672.5341	−18.3
2 449 673.5209	−22.2
2 449 674.5146	−20.8
2 449 675.5215	−18.5
2 449 676.5149	−21.6
2 449 678.5130	−19.9
2 449 679.5442	−22.0

Each echelle order had the continuum fitted and removed by a 5 piece cubic spline and the spectra were rebinned to 2048 bins before the actual cross-correlation.

Extensive tests were performed to find the best wavelength range and to choose the optimal parameters for the filtering of the Fourier spectrum. We found that the best wavelength region was 410–555 nm so this region was used for the last (1994) run, whereas for the earlier runs only the region 475–555 nm was employed. The best filter turned out to ramp up from wavenumber 30 to 40 and taper off from 350 to 400.

In general the twilight sky exposure gave the best cross-correlation peak due to a better signal-to-noise ratio, and 47 Tuc-C349 was used to determine nightly velocity offsets. For the early data a reference velocity of -21.5 ± 0.2 km s^{-1} was adopted on the basis of the average values from the 1989 run itself and from same-epoch CORAVEL data (see Storm et al. 1991). The mean radial velocity for the 1994 run came out as -20.8 ± 0.6 km s^{-1} for 47 Tuc-C349 but this is mostly due to a different selection of wavelength range. Using the same wavelength range as the previous years gave -21.8 km s^{-1}. As we are interested in the best possible relative velocities between the different observing runs we have adopted the value of -21.5 km s^{-1} as the reference velocity and applied nightly shifts to all the nights to bring all the velocities on the same system.

All velocities are referred to the barycenter of the solar system using the facility within `XCSAO` for transferring the observed velocities to this reference frame.

The final velocities were determined from weighted means of the velocities determined for the individual orders. The typical standard deviation for a single order is 3 km s^{-1} and using 10 or 20 orders thus brings down the formal error on the mean to well below 1 km s^{-1}. To this error has to be added the error on the nightly shifts as determined from the observations of C349. This error can be estimated from the standard deviations from the mean and is of the order 1.4 km s^{-1} which should be added quadratically to the internal formal error. Realistic errors can also be estimated from the radial velocity curves themselves (see Fig. 9) by determining the spread around a smooth curve.

Table 7. Intensity mean magnitudes and colors based on the combined datasets for each star in the sample.

ID	$\langle V\rangle$	$\langle B\rangle-\langle V\rangle$	$\langle V\rangle-\langle R\rangle$	$\langle V\rangle-\langle I\rangle$	$\langle V\rangle-\langle K\rangle$	$\langle J\rangle-\langle K\rangle$	$\langle W\rangle$
HV 822	14.523	0.769	0.409	0.861	1.903	0.482	12.362
HV 1328	14.116	0.566	0.364	0.678	1.538	0.407	12.413
HV 1333	14.707	0.712	0.432	0.839	1.905	0.472	12.601
HV 1335	14.808	0.648	0.440	0.798	1.823	0.419	12.805
HV 1345	14.763	0.694	0.397	0.800	1.924	0.499	12.756

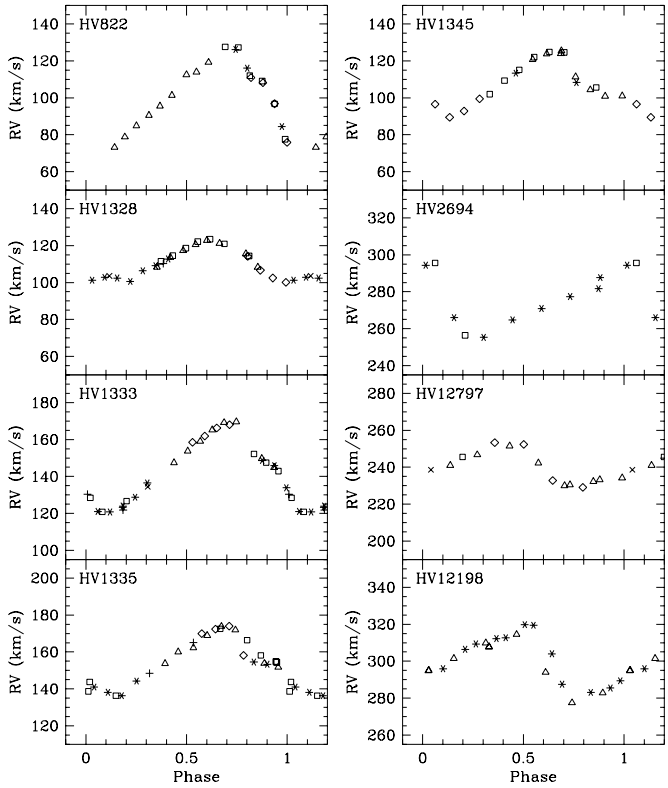

Fig. 9. Radial velocity curves for the Cepheids. Note that the radial velocity scale is the same in all the frames. The data are labelled according to the run they were aquired. Open boxes are from 1987, open diamonds 1988, open triangles 1989, asterisks 1994 and crosses and plusses are NTT data from 1992 and 1993 respectively. The three last stars are LMC stars.

We estimate a standard error of 1.5–2.0 km s^{-1} per observation which is also in good agreement with the computed value.

The velocities are listed in Table 25 and 26 together with the Heliocentric Julian Dates (HJD) at mid-exposure. In Fig. 9 the radial velocity curves resulting from these observations and adopting the ephemerides from Table 4 are plotted.

A few measurements for HV 821 and HV 883 were obtained as well and they are listed in Table 27.

5. Observational parameters

In Table 7 we summarize the integrated properties of the stars. The magnitudes are all intensity magnitude averages. To assure the best possible phase coverage and optimal definition of the mean magnitudes we have performed the V and I averages over the data presented here combined with the Udalski et al. (1999) data for HV 822, HV 1335, and HV 1345, and the Caldwell & Coulson (1984) data, offset by +0.07 mag in V, for HV 1335. The reddening-insensitive Wesenheit index, $\langle W\rangle$, defined as $\langle W\rangle = \langle V\rangle - 2.51(\langle V\rangle - \langle I\rangle)$ where sharp brackets indicates intensity averages, has been tabulated as well.

Table 8. The Fourier coefficients for the V light curves for the SMC Cepheids.

ID	A_1 mag	k	R_{k1}	$\sigma(R_{k1})$	ϕ_{k1}	$\sigma(\phi_{k1})$
HV 822	0.41	2	0.31	0.04	4.51	0.12
		3	0.18	0.04	2.58	0.23
		4	0.11	0.03	1.15	0.36
HV 1328	0.32	2	0.19	0.02	4.33	0.10
		3	0.14	0.02	1.58	0.14
		4	0.11	0.02	5.28	0.17
HV 1333	0.38	2	0.37	0.04	4.88	0.15
		3	0.22	0.05	2.79	0.22
		4	0.26	0.04	1.42	0.24
HV 1335	0.34	2	0.30	0.04	4.39	0.18
		3	0.13	0.04	1.35	0.39
		4	0.08	0.04	5.33	0.51
HV 1345	0.32	2	0.20	0.04	4.49	0.18
		3	0.18	0.04	1.87	0.22
		4	0.15	0.04	5.50	0.26

We have also computed the Fourier parameters $R_{21}-R_{41}$ and $\phi_{21}-\phi_{41}$ (as defined by Petersen (1986)) for the Cepheids based on the V light curves using $N = 4$, i.e. four components. The resulting parameters are tabulated in Table 8 together with the associated error estimates. The semi-amplitudes for the first (A_1) order are also tabulated. Table 9 contains the same parameters but derived for the radial velocity curves and following the convention from Simon (1988) where the radial velocity coefficients are based on a sine series, which means that the phases are shifted by $\pi/2$ with respect to the cosine series used for the photometric data.

The photometric amplitude ratios R_{21} are in good agreement with the values found by Udalski et al. (1999) for their large sample of SMC stars.

Pont et al. (2001) have obtained accurate radial velocity curves for a sample of Galactic cepheids at relatively large Galactocentric distances with expected lower-than-solar metallicities. They find weak evidence that the ϕ_{21} parameter is metallicity-sensitive for periods longer than about 12 days as the star HW Pup exhibits a significantly larger ϕ_{21} than that

Table 9. The Fourier coefficients for the radial velocity curves for the SMC Cepheids.

ID	A_1 km s^{-1}	k	R_{k1}	$\sigma(R_{k1})$	ϕ_{k1}	$\sigma(\phi_{k1})$
HV 822	27	2	0.25	0.03	2.89	0.14
		3	0.09	0.03	4.62	0.32
		4	0.14	0.03	0.42	0.24
HV 1328	11	2	0.19	0.02	4.17	0.12
		3	0.10	0.02	0.14	0.21
		4	0.08	0.02	2.31	0.27
HV 1333	22	2	0.13	0.02	2.93	0.18
		3	0.08	0.02	3.63	0.27
		4	0.09	0.02	0.17	0.26
HV 1335	16	2	0.06	0.05	3.05	0.86
		3	0.13	0.05	3.23	0.42
		4	0.11	0.05	0.23	0.46
HV 1345	15	2	0.18	0.05	5.40	0.28
		3	0.22	0.05	2.54	0.26
		4	0.07	0.05	5.94	0.70

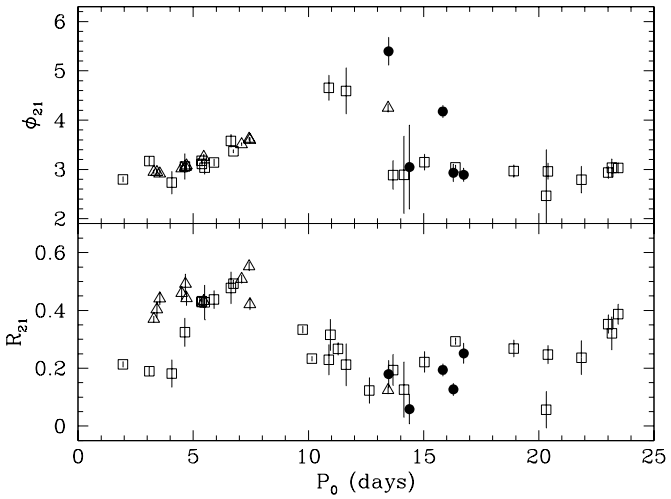

Fig. 10. The radial velocity Fourier parameters for our program stars (filled circles), a solar metallicity Galactic sample (open squares), and the low metallicity Galactic sample of Pont et al. (2001) (open triangles).

found for solar-metallicity Cepheids. HW Pup with a period of 13.5 days is indeed metal-poor, with [Fe/H] = −0.29 according to Andrievsky et al. (2002) and −0.51 according to de Almeida (priv. comm.).

To further investigate this possibility we have overplotted the data from Pont et al. (2001) in Fig. 10 with our data and data from a sample of nearby galactic stars with good radial velocity curves (see the companion paper Storm et al. 2004). We see that a couple of our stars exhibit an even higher value of ϕ_{21} than Pont et al. (2001) found for HW Pup. However, we also have three SMC stars which are in good agreement with the supposedly solar metallicity galactic sample. A clarification of this question will have to await individual spectroscopic metallicities for these stars, and possibly also a larger sample.

Acknowledgements. We appreciate the help we have received from Laura Kellar Fullton and Ricardo Muñoz in collecting the photometric data. BWC thanks the U. S. National Science Foundation for grants AST-8920742 and AST-9800427 to the University of North Carolina for support of this research. WPG acknowledges support for this work from the Chilean FONDAP Center for Astrophysics 15010003. Thanks is also due to Jørgen Otzen Petersen who kindly provided his IDL program to compute the Fourier coefficients and to the staff of the three observatories where the data were obtained.

References

Andrievsky, S. M., Kovtyukh, V. V., Luck, R. E., et al. 2002, A&A, 392, 491
Caldwell, J. A. R., & Coulson, I. M. 1984, SAAO Circ., 8, 1
Chun, M. S., & Freeman, K. C. 1978, AJ, 83, 376
Freedman, W. L., Madore, B. F., Gibson, B. K., et al. 2001, ApJ, 553, 47
Fouqué, P., & Gieren, W. P. 1997, A&A, 320, 799
Hodge, P. W., & Wright, F. W. 1977, The Small Magellanic Cloud (Seattle: Univ. of Washington Press)
Kurtz, M. J., Mink, D. J., Wyatt, W. F., et al. 1992, PASPC 25, ed. D. M. Worral, C. Biemesderfer & J. Barnes, 432
Landolt, A. U. 1992, AJ, 104, 340
Laney, C. D., & Stobie, R. S. 1994, MNRAS, 266, 441
Morse, J. A., Mathieu, R. D., & Levine, S. E. 1991, AJ, 101, 1495
Persson, S. E., Murphy, D. C., Krzeminski, W., Roth, M., & Rieke, M. J. 1998, AJ, 116, 2475
Petersen, J. O. 1986, A&A, 170, 59
Pont, F., Kienzle, F., Gieren, W., & Fouqué, P. 2001, A&A, 376, 892
Schecter, P. L., Mateo, M., & Saha, A. 1993, PASP, 105, 1342
Simon, N. R. 1988, in Pulsation and Mass Loss in Stars, ed. R. Stalio, L. A. Willson (Dordrecht: Kluwer), Astrophys. Space Sci. Lib., 148, 27
Stetson, P. B. 1987, PASP, 99, 191
Storm, J., Carney, B. W., Freedman, W. L., & Madore, B. F. 1991, PASP, 103, 261
Storm, J., Carney, B. W., & Fry, A. M. 1998, in Views on Distance Indicators, ed. M. Arnaboldi, F. Capuot & A. Rifatto, Mem. Soc. Ast. It., 69, 79
Storm, J., Carney, B. W., & Fry, A. M. 1999, in Harmonizing Cosmic Distance Scales in a Post-HIPPARCOS Era, ed. D. Egret & A. Heck, ASP. Conf. Ser., 167, 320
Storm, J., Carney, B. W., Gieren, W. P., Fouqué, P., & Fry, A. M. 2000, in The Impact of Large-Scale Surveys on Pulsating Star Research, ed. L. Szabados & D. Kurtz, ASP Conf. Ser., 203, 145
Storm, J., Carney, B. W., Gieren, W. P., et al. 2004, A&A, 415, 531
Tonry, J. L., & Davis, M. 1979, AJ, 84, 1511
Udalski, A., Soszyński, I., Szymański, M., et al. 1999, Acta Astr., 49, 437
Welch, D. L., McLaren, R. A., Madore, B. F., & McAlary, C. W. 1987, ApJ, 162, 1987